Photophysics and Rotational Dynamics of a β-Carboline Analogue in Nonionic Micelles: Effect of Variation of Length of the Headgroup and the Tail of the Surfactant

ARTICLE *in* THE JOURNAL OF PHYSICAL CHEMISTRY B · JUNE 2009

Impact Factor: 3.3 · DOI: 10.1021/jp900575e · Source: PubMed

Photophysics and Rotational Dynamics of a β-Carboline Analogue in Nonionic Micelles: Effect of Variation of Length of the Headgroup and the Tail of the Surfactant

Atanu Mahata, Deboleena Sarkar,* Debosreeta Bose, Debanjana Ghosh, Agnishwar Girigoswami, Paramita Das, and Nitin Chattopadhyay*

Department of Chemistry, Jadavpur University, Kolkata 700032, India

Received: January 20, 2009; Revised Manuscript Received: April 13, 2009

Effect of variation of length of nonionic surfactants in terms of the headgroup as well as the tail part on the photophysical and rotational dynamical properties of a β-carboline analogue, 3-acetyl-4-oxo-6,7-dihydro-12*H*-indolo-[2,3-*a*]quinolizine (AODIQ) has been investigated. Steady-state and time-resolved fluorescence and fluorescence anisotropy have been exploited for the purpose. The experiments revealed modification of the photophysics of AODIQ by the conjugate effect of polarity and rigidity of the micellar environments with varying poly(ethylene oxide) chain length in the case of Triton X series and the alkyl chain length in the case of Tween series surfactants. Fluorometric studies suggest that the fluorophore resides at the micelle−water interface in all these systems. The enhancements in the steady-state anisotropy in all the micellar media compared to those in pure aqueous solution reflect that the fluorophore is located in motionally restricted regions introduced by the nonionic micelles. Contrary to the single exponential nature of the fluorescence anisotropy decay of AODIQ in aqueous medium, they were found to be biexponential in the micellar environments. The rotational relaxation of AODIQ in the micellar environments has been discussed in light of the *two-step and wobbling in a cone* model. The model helps to evaluate different rotational parameters and to ascertain the location of the fluorophore in the micellar media. The significant feature is that the motional restriction decreases with an increase in the poly(ethylene oxide) chain length while it increases with an increase in the alkyl chain length. The difference in the extent of water penetration due to variation in the thickness of the palisade layer and therefore a variation in the micellar polarity with a variation of the length of poly(ethylene oxide) and alkyl chain has been argued to be responsible.

1. Introduction

Amphiphilic surfactant molecules capable of forming micelles, the dynamic nanostructures, are drawing serious attention from chemists due to their importance as catalysts and solubility enhancers of a wide range of organic molecules.[1,2] Interactive feature of innumerous fluorophores in micellar systems have been studied because of the fact that micelles, in a simple model, mimic the membranes of biosystems.[3,4] Micellar activity toward the thermodynamics and kinetics of different photophysical processes has been extensively studied.[5−7] Interest on this aspect has resulted in an explosive growth in research on various bioactive molecules.[5−7] Recent studies throw light on the interaction of bioactive fluorophores with the surfactants and pay attention to the binding of the probes with the micelles and distribution and/or location of them within the micellar environments.

Aqueous micellar environments modify a number of photophysical/photochemical processes because of a change in the micropolarity and rigidity inside the micellar microenvironments compared to the situation in the bulk aqueous phase. It is now fairly well understood that the rates of many chemical reactions, especially those of the processes like charge transfer, electron transfer, etc. are largely influenced by the microenvironment surrounding the reacting species. The interaction of an intramolecular charge-transfer (ICT) fluorophore with the micelles allows one to investigate the distribution and location of the probe in the micelles. Such studies are modeled to understand the interaction, distribution, and localization of bioactive fluorophores in biological systems. The ICT process has also been exploited to investigate different aspects of micellar microenvironments like critical micellar concentration (CMC), micropolarity, microviscosity, aggregation properties, etc. In a micellar environment the ICT process is largely modified, controversially, due to either the reduction in polarity or enhanced steric constraint, leading to a marked change in the fluorescence yield, fluorescence lifetime and fluorescence anisotropy of the CT emission.[8] To ascertain that the probe is located in the target environment, various probe properties like the position, intensity, and shape of the absorption and/or fluorescence bands, can be compared to those in the bulk-phase systems that simulate the conditions in the microenvironments.[8−10]

A direct consequence of an organized molecular assembly is the restriction imposed on the dynamics and mobility of the constituent structural units. Depolarization of the fluorescence of the probe has been established to be the most sensitive and powerful technique to elucidate the dynamical information about the fluorophore in the complex microheterogeneous environments like micelles, reverse micelles, lipids, cyclodextrins, etc.[11−15] Ionic or polar probes usually provide an opportunity to study the dynamics in fairly well-defined aqueous micelles. The presence of a large number of heteroatoms in such probes facilitate in their localization in the micelle−water interfacial region. Dynamical information includes tumbling or rotational motion of the bound fluorophore within the microheterogeneous environments on the picosecond/nanosecond time scale.[16] In

* Corresponding authors. Fax: 91-33-2414-6266. E-mails: debbierims@yahoo.co.in (D.S.), nitin.chattopadhyay@yahoo.com (N.C.).

10.1021/jp900575e CCC: $40.75
Published on Web 05/05/2009

SCHEME 1: Structure of (a) Triton X and (b) Tween Surfactants

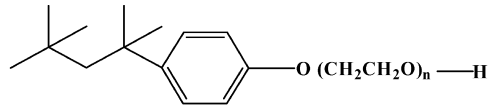

(a)

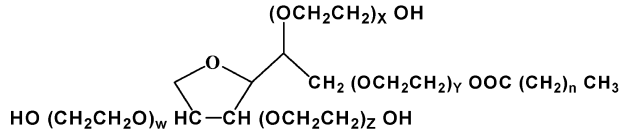

(b)

general, the rotational diffusion coefficient is inversely related to the viscosity of the solvent by the Stokes−Einstein equation for neutral molecules. In microheterogeneous media the rotational dynamics of a dye is fundamentally different from that in the homogeneous media in two aspects. Firstly, the existence of an aqueous/nonaqueous interface leads to an orientationally nonrandom equilibrium distribution of the molecules and secondly, the molecular dynamics is highly restricted. Understanding the rotational dynamics of a probe in microheterogeneous media is thus highly significant for the interpretation of the dynamics of drugs in biological systems.

With this perspective we intended to investigate the effects of nonionic surfactants with a variation in the chain length of the headgroup and the tail part on the micellar behavior. Several papers on nonionic micelles have been presented addressing to the structural aspect including size, shape, and hydration of the micelle in relation to the poly(ethylene oxide) and alkyl chain length.[17,18] However, water−micelle interactions are still foggy, especially in the case of nonionic surfactants. Our attempt in the present work was to probe the palisade layer in a series of nonionic surfactants and decipher how the interactions vary with a change in the poly(ethylene oxide) chain length and alkyl chain length. The thickness and hydration of the palisade layer are expected to vary as these chain lengths are tuned. Our objective was to probe the pattern of this variation. For the purpose we used two separate homologous series of nonionic surfactants, the Triton X series (with varying poly(ethylene oxide) chain length) and the Tween series (with varying alkyl chain length) (Scheme 1).

The Triton X family, a trademark of Rohm and Haas,[25] is the group of detergents all containing a *p-tert*-octylphenyl (OP) hydrophobic moiety with a poly(ethylene oxide) (PEO) chain constituting the hydrophilic part. The Triton X series of surfactants studied here are Triton X-114 (OP + 7.5 PEO), Triton X-100 (OP + 9.5 PEO), and Triton X-165 (OP + 16 PEO). The Tween family comprises 20 poly(ethylene oxide) hydrophilic headgroups with different alkyl chain lengths. Tweens selected for the present study are Tween 20 (12 carbon chain length), Tween 40 (16 carbon chain length), and Tween 60 (18 carbon chain length). The relevant micellar parameters are listed in Table 1.

The fluorophore used to probe these micellar environments is a potentially bioactive β-carboline derivative, namely, 4-oxo-6,7-dihydro-12*H*-indolo-[2,3-*a*]-quinolizine (AODIQ). It possesses dual emission from viz., a locally excited (LE) state and a charge-transfer (CT) state.[19] The polarity sensitive CT emission of AODIQ enables us to exploit it successfully for demonstrating and characterizing various bio- and biomimetic microenvironments.[8,11,20−23] It has also been exploited as an effective fluorosensor for sensing essential trace metals under suitable environmental conditions.[24] Entrapping of such biologically potent molecules with different biomimetic environments attracts interest of the researchers to explore the potential usefulness of its fluorescence properties for the understanding of its interaction with relevant biological targets.

TABLE 1: Micellar Parameters in Triton X and Tween Micelles

surfactants	*n*	CMC (mM)	aggregation no.	HLB[a]	ref
Triton X-114	7.5	0.210	189	12.0	25, 26
Triton X-100	9.5	0.250	146	14.0	25, 26
Triton X-165	16	0.430	82	16.0	25, 26
Tween-20	10	0.050	86	16.7	27, 28
Tween-40	14	0.023	90	14.9	27, 28
Tween-60	16	0.021	110	11.0	27, 28

[a] Hydrophilic lipophilic balance.

SCHEME 2: Structure of AODIQ

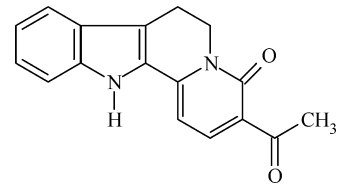

2. Experimental Section

3-Acetyl-4-oxo-6,7-dihydro-12*H*-indolo-[2,3-*a*]-quinolizine (AODIQ) (Scheme 2) was synthesized using the method mentioned elsewhere.[29] It was purified by column chromatography, and the purity of the compound was checked by thin layer chromatography (TLC). The compound was further vacuum sublimed before use. Triton X-114, Triton X-100, and Triton X-165 (Sigma-Aldrich) and Tween-20, Tween-40, and Tween-60 (Merck) were used as received without further purification. All the solvents used were of UV spectroscopic grade (Spectrochem). Triply distilled water was used for making the experimental solutions. The concentration of AODIQ was kept at 3×10^{-6} M throughout the experiment.

Absorption and steady-state fluorescence measurements were performed using a Shimadzu MPS 2000 spectrophotometer and a Spex fluorolog II spectrofluorometer, respectively. The steady-state fluorescence anisotropy was measured with a Perkin-Elmer LS55 spectrofluorometer. Steady-state anisotropy, *r*, is defined by

$$r = (I_{VV} - GI_{VH})/(I_{VV} + 2GI_{VH}) \quad (1)$$

where I_{VV} and I_{VH} are the intensities obtained with the excitation polarizer oriented vertically and the emission polarizer oriented

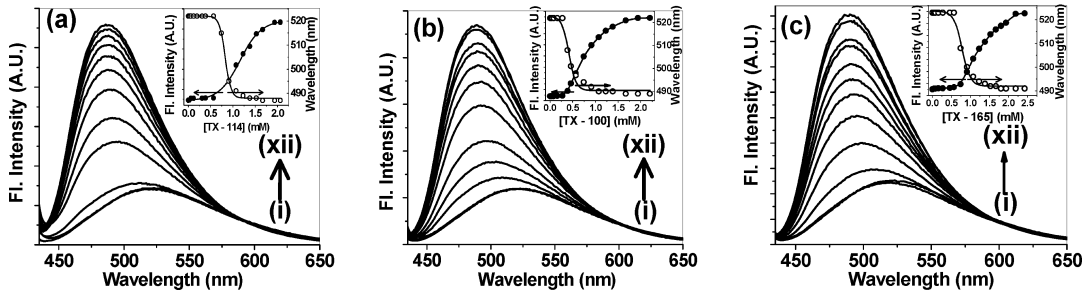

Figure 1. Emission spectra of AODIQ (3×10^{-6} M) solution with added (a) TX-114, (b) TX-100, and (c) TX-165 ($\lambda_{ex} = 420$ nm). Curves correspond to 0, 0.16, 0.3, 0.5, 0.6, 0.75, 0.9, 1.0, 1.23, 1.4, 1.7, and 2.0 mM TX-114 in (a), 0, 0.16, 0.3, 0.5, 0.6, 0.75, 0.9, 1.0, 1.23, 1.4, 1.7, and 2.0 mM TX-100 in (b), 0, 0.15, 0.5, 0.75, 1.0, 1.23, 1.4, 1.7, 1.8, 1.9, 2.2, and 2.5 mM TX-165 in (c). Insets show the variations of the fluorescence intensities and wavelength against the surfactant concentrations.

vertically and horizontally, respectively. The G factor was defined as

$$G = I_{HV}/I_{HH} \tag{2}$$

where I terms denote parameters similar to those mentioned above for the horizontal position of the excitation polarizer. Quantum yields were determined using quinine sulfate in 0.1 N H_2SO_4 ($\varphi_f = 0.54$).[30] Fluorescence lifetimes were determined from time-resolved intensity decays by the method of time-correlated single-photon counting using a picosecond diode laser at 403 nm (IBH, nanoLED-07) as the light source and TBX-04 as the detector, and the signals were collected at a magic angle of 54.7°. The decays were deconvoluted using IBH DAS-6 decay analysis software. The goodness of fits was evaluated by χ^2 criterion and visual inspection of the residuals of the fitted function to the data. Mean (average) fluorescence lifetimes (τ_f) for the biexponential fittings were calculated from the decay times (τ) and the pre-exponentials (a) using the following relation

$$\langle\tau_f\rangle = \sum a_i\tau_i^2/\sum a_i\tau_i \tag{3}$$

For anisotropy decay measurements, the samples were excited at 403 nm using a picosecond diode laser (IBH) and a Hamamatsu microchannel plate photomultiplier tube (3809U). The instrument response function (fwhm) of the setup was 90 ps. For the anisotropy decays, we used a motorized polarizer in the emission side. The emission intensities at parallel ($I_{||}$) and perpendicular ($I_{\perp}$) polarizations were collected alternatively until a preset peak difference was reached. The preset value, however, depended on the tail matching of the parallel and perpendicular decays. Logically, the technique might fail for extremely slow tumbling motion of the fluorophore introduced by some very rigid microenvironment. For normal micellar systems like the present ones, however, the method works quite well. Furthermore, to combat with a relatively bigger micellar system, the preset value of the peak difference is often enhanced.[4,10,13,48] To improve the signal-to-noise ratio, the data sets were averaged together. The analysis of the data was done using IBH DAS, version 6, decay analysis software. Each τ_i in the multiexponential total intensity decay was associated with each τ_{fi} in the multiexponential expression of the anisotropy. The quality of the fit was determined from the reduced χ^2 and by visual inspection of the fit and the data. The time-resolved anisotropy [$r(t)$] was calculated using the following relation

$$r(t) = [I_{||}(t) - GI_{\perp}(t)]/[I_{||}(t) + 2GI_{\perp}(t)] \tag{4}$$

where G is the correction factor for the detector sensitivity to the polarization detection of the emission.[31] Average rotational relaxation times (τ_r) for the biexponential iterative fittings were calculated from the decay times (τ_{1r} and τ_{2r}) and the relative amplitudes (a_{1r} and a_{2r}) using the following relation

$$\langle\tau_r\rangle = a_{1r}\tau_{1r} + a_{2r}\tau_{2r} \tag{5}$$

For the dynamic light scattering (DLS) measurements, we used a Malvern Nano-ZS instrument employing a 4 mW He−Ne laser ($\lambda = 632.8$ nm) and equipped with a thermostated sample chamber using DTS software. The sample was poured into a DTS0112 low volume disposal sizing cuvette of 1.5 mL (path length 1 cm). The operating procedure was programmed in such a way that there were averages of 25 runs, each run being averaged for 15 s and then a particular hydrodynamic diameter and size distribution was evaluated using the DTS software. All experiments were carried out at 173° scattering angle.

All the experiments were performed at 25 °C with air-equilibrated solutions.

3. Results and Discussion

In water AODIQ shows a broad low energy absorption band with maximum at 420 nm,[19] which shows about 4 nm red shift in all the Triton X and Tween micelles. This indicates that the ground state of AODIQ experiences a lower polarity in the micellar environments.

Upon addition of the nonionic surfactants, in all the cases the fluorophore shows a blue shift in the emission maximum from 520 nm in water[19] together with a large enhancement in the fluorescence quantum yield. Figures 1 and 2 show the fluorescence spectra of AODIQ in the different micellar media.

Insets of Figures 1 and 2 show the variations of the fluorescence intensities and fluorescence maxima of AODIQ as a function of surfactant concentration and allow one to determine the critical micellar concentrations (CMC) of the individual systems. The CMC values in the present case for all the surfactants correspond well with the literature reports.[26−29]

A comparison of the observed blue shift in the fluorescence maximum and an increase in the fluorescence quantum yield of AODIQ in microheterogeneous environments to that in aqueous solution suggests that the microenvironments around the fluorophore in the micellar solutions are quite different from the pure aqueous phase. The blue shift indicates that the polarity of the micellar environment is less than the polarity of the bulk water since a similar blue shift is observed in homogeneous solvents of lower polarity.[19] It is also important to note that the CT emission band of AODIQ becomes narrower in the micellar media compared to that in aqueous solution, pointing further to the probe−micelle interaction. Similar narrowing of the CT

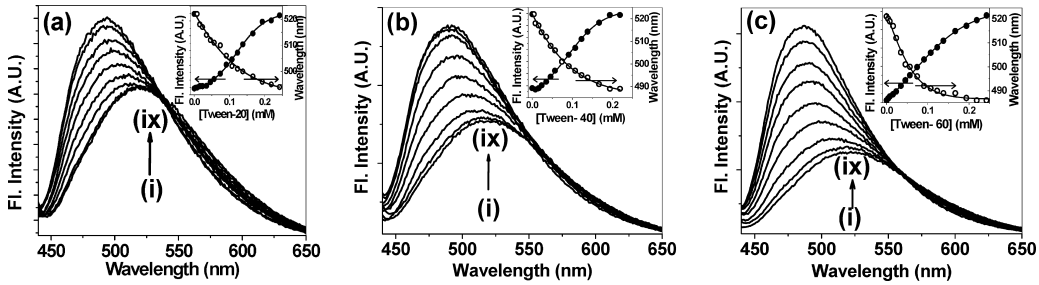

Figure 2. Emission spectra of AODIQ (3×10^{-6} M) solution with added (a) Tween-20, (b) Tween-40, and (c) Tween-60 ($\lambda_{ex} = 420$ nm). Curves correspond to 0, 0.016, 0.05, 0.075, 0.1, 0.15, 0.2, and 0.25 mM Tween-20 in (a), 0, 0.008, 0.016, 0.035, 0.06, 0.09, 0.123, 0.17, and 0.22 mM Tween-40 in (b), 0, 0.008, 0.016, 0.035, 0.06, 0.09, 0.123, 0.17, and 0.22 mM Tween-60 in (c). Insets show the variations of the fluorescence intensities and wavelength against the surfactant concentrations.

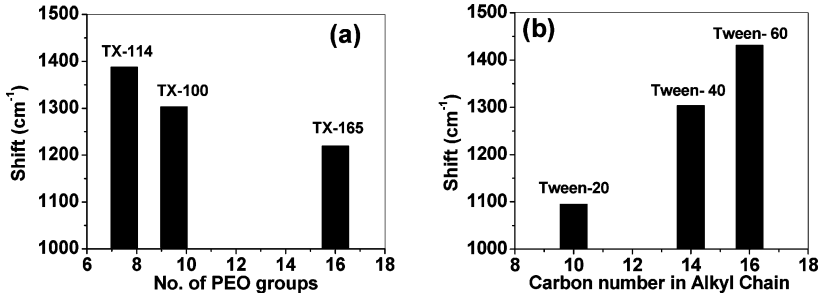

Figure 3. Variation of the shift in energy corresponding to the emission maxima with number of carbon atoms in the (a) poly(ethylene oxide) chain in Triton X micelles and (b) alkyl chain in Tween micelles.

band of AODIQ was also observed in other microheterogeneous environments in our previous studies.[20−23]

For a better realization of the effect of poly(ethylene oxide) (PEO) and alkyl chain length on the spectral behavior of AODIQ a bar diagram has been presented in Figure 3 showing the shift in the emission maxima in different micelles from that observed in aqueous solution. It is evident from the figure that the hypsochromic shift in the case of Triton X series increases as the PEO chain length decreases (maximum for TX-114 with the shortest PEO chain length) and that in the Tween series increases with an increase in alkyl chain length (maximum for Tween-60 with longest chain length). Therefore it can be inferred that the probe experiences a less polar environment as the PEO chain length decreases and/or the alkyl chain length increases.

When a chromophore is dissolved in a micellar medium, the local environment becomes rather complex. As the properties of the core and the headgroup regions are different, the fluorophore can reside either in the core or in the interface region or may be distributed within these two distinct regions depending on the polarity/charge characteristics of both the probe and the micelle. The polarity determined through different photophysical parameters of the probe gives a relative measure of the polarity of the microenvironment next to the probe. Local polarity around a probe in biomimetic environments may be estimated by comparison of the spectral properties of the fluorophore in the environment with those of the probe in pure solvents or solvent mixtures of known polarities.[8,11,19−23,31,32] It is often argued that the polarities of the homogeneous and microheterogeneous media are not exactly the same. However, a relativistic estimate of polarity of such environments is commonly made through such measurements. For the purpose, people use various scales of polarity like the Lippert−Mataga scale, equivalent $E_T(30)$ scale, etc.[33] Kumbhakar *et al.* recently determined the micropolarity around coumarin 153 in TX-100 and TX-165 micelles using the Lippert−Mataga scale.[9] They suggested that the fluorophore resides in the palisade regions of both TX-165 and TX-100 micelles and the palisade layer of the former is more polar than the latter.[9] For the present study we have used the $E_T(30)$ scale of polarity.[33,34]

The $E_T(30)$ values of the water−dioxane mixtures were collected from the literature.[35] A typical calibration curve thus obtained from a plot of fluorescence maximum of AODIQ in water−dioxane mixtures against corresponding $E_T(30)$ of the solutions establishes a linear correlation between the two, as indicated in Figure 4. Interpolating the values of the emission maxima of AODIQ bound to the micelles at the saturation level of probe-micelle interactions on the above correlation, we have determined the micropolarity values around the probe and they are tabulated in Table 2.

The micropolarities around AODIQ in micellar environments are close to the micropolarity of ∼65−70% of the dioxane−water mixture. It is pertinent here to justify the choice of water/dioxane mixture over water/alcohol that is often used for similar studies. We have observed that the emission maximum of AODIQ in the micellar media is very close to that in methanol solvent. Thus, use of a methanol/water solvent mixture for generating the polarity calibration curve will be unreliable for the determination of the micropolarity around the fluorophore in the present case, since the determined polarity falls at an end of the calibration curve. Use of other alcohols does not improve the situation very much. However, use of dioxane/water mixture covers a much wider range of polarity and is thus free from this difficulty. Estimated micropolarities in the micellar media suggest that the fluorophore resides in micelle water interface as the polarity values differ widely from those in bulk water ($E_T(30) = 63.1$[34]) and in nonpolar hydrocarbon core (e.g., $E_T(30) = 31.1$ for *n*-heptane[34]).

A close inspection of the $E_T(30)$ values leads to the inference that polarity in TX-165 is highest among the Triton X series and least in TX-114, consistent with the observation of Kumbhakar *et al.* using a different probe.[9] In the case of the Tween series, we find that the microenvironment is least polar in the case of Tween-60 and most polar in the case of Tween-

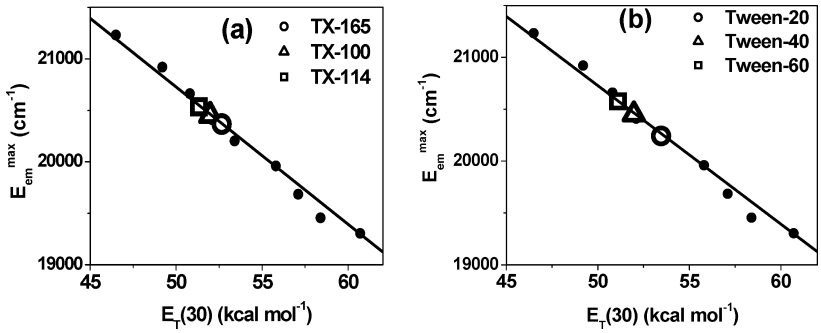

Figure 4. Variation of energies corresponding to the emission maximum (E_{em}^{max}) of AODIQ in a dioxane−water mixture against $E_T(30)$. The concentration of AODIQ is kept at 3×10^{-6} M. The open symbols give the interpolated energies corresponding to the fluorescence maxima values in (a) Triton X series of micelles and (b) Tween series of micelles.

TABLE 2: $E_T(30)$ and Stern−Volmer Quenching Constant Values of AODIQ in Aqueous and Nonionic Micellar Media

environment	$E_T(30)$ (kcal mol^{-1})	$10^{-3}K_{SV}$ (L mol^{-1})
water	63.1[a]	25.3
TX-114 (2.0 mM)	51.3	6.5
TX-100 (2.2 mM)	52.0	7.0
TX-165 (2.5 mM)	52.7	8.2
Tween-20 (0.25 mM)	53.5	1.3
Tween-40 (0.20 mM)	52.4	1.2
Tween-60 (0.20 mM)	51.3	1.0

[a] From ref 34.

20 (see Table 2). This shows that an increase in the PEO chain provides a more polar environment while the reverse occurs with an increase in the alkyl chain length. The increase in alkyl chain length increases micellar compactness.[36] Micelles with compact headgroups suffer a smaller water penetration compared to the micelles with less compact headgroups. Thus the fluorophore experiences more rigid and less polar environments from Tween-20 to Tween-60 through Tween-40. Upon increasing the PEO chain length, however, micelles suffer greater water penetration due to reduced compactness of the micelles. Hence polarity increases in the order TX-114 < TX-100 < TX-165.

Metal Ion Induced Fluorescence Quenching. Quenching of the fluorescence of micelle-bound AODIQ by the external heavy metal ion has been studied using ionic quencher Cu^{2+} with an intention to see the degree of accessibility of the fluorophore in different surfactant media toward the quencher and hence to see the impact of variation of surfactant chain length (both PEO and alkyl chain length) on the degree of exposure of the probe.[24,31] The idea behind the experiment is the following. The ionic quencher is not supposed to be available in the micellar core due to the very low polarity in the said region. It is expected to be available in aqueous phase as well as in the micelle−water interface.[8] Hence, had the fluorophore been located into the micellar core, there would have been inappreciable fluorescence quenching due to the lack of availability of the quencher (Cu^{2+}). However, observation of a perceptible quenching in the micellar environments strongly suggests that the probe is not located in the micellar core. The quenching of the fluorescence of AODIQ with the addition of quencher (Cu^{2+}) followed the Stern−Volmer relation where the terms have their usual meanings:

$$F_0/F = 1 + K_{SV}[Q] \quad (6)$$

Figure 5 depicts the Stern−Volmer plots for the quenching of AODIQ fluorescence in all the micellar environments. The slope of each plot gives the Stern−Volmer quenching constant (K_{SV}). The higher the slope, the more efficient the quenching is and the greater is the degree of exposure of the probe to Cu^{2+}. The quenching of AODIQ in all the micellar environments studied is significantly less than that in the pure aqueous phase, implying lesser accessibility of the probe to the quencher within the micellar media as compared to the aqueous phase. With an increase in the PEO chain length the K_{SV} values are found to increase, having the maximum value in TX-165 with the longest PEO chain (Figure 5a). On the contrary, the K_{SV} attains a minimum value for Tween-60 having the longest alkyl chain length (Figure 5b).

The relative magnitude of the fluorescence quenching efficiency with an increase in the chain length of the surfactants constituting the micelles can be rationalized in terms of the compactness of the headgroups and water penetration within the micelles. It is known that water can enter micelles up to a certain depth depending on the compactness of the micellar units.[31,37,38] As mentioned in the previous section, compact micelles suffer smaller water penetration. As we increase the alkyl chain length (as in the Tween series of surfactants), the increased chain length enhances the compactness of the micelle, leading to a decrease in the water penetration. On the other hand, polarity in the palisade layer increases with an increase in the PEO chain length, leading to an increase in water penetration within the Triton X micelles. Thus, the accessibility of the fluorophore toward the quencher is controlled by both the PEO and the alkyl chain length; thereby changing the K_{SV} value accordingly.

Steady-State Fluorescence Anisotropy. Measurement of fluorescence anisotropy provides significant information about the physical characteristics and the nature of the environment of fluorescent probes.[31] An increase in the rigidity of the environment surrounding the fluorophore results in an increase in the fluorescence anisotropy. Figure 6 depicts the variation of fluorescence anisotropy of AODIQ as a function of concentration of the nonionic micelles studied here. It reflects the degree of rigidity imposed on the probe in different micellar media. The observations can be explained from the consideration of the compactness of the micelles.[4,36]

Micelles having a compact headgroup are more rigid in nature and allow minimum water penetration. Compactness of headgroups increase with an increase in alkyl chain length and decreases with an increase in the PEO chain length.[37,38] Thus the fluorophore experiences a more rigid micellar environment in the order TX-165 < TX-100 < TX-114 within the Triton X series and Tween-20 < Tween-40 < Tween-60 within the Tween series. The observation corroborates the findings from the micropolarity determination and quenching experiments as discussed above.

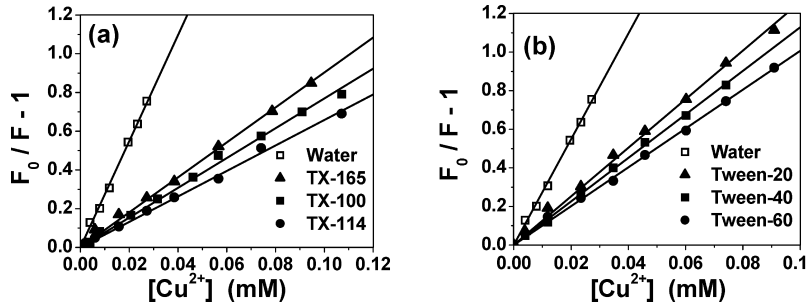

Figure 5. Stern−Volmer plots for the fluorescence quenching of AODIQ by Cu^{2+} ions in aqueous micellar solutions in the case of (a) Triton X series and (b) Tween series of surfactants.

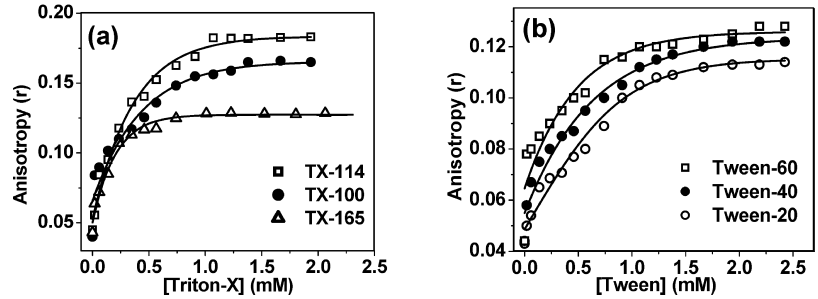

Figure 6. Variation of the fluorescence anisotropy (r) of AODIQ (3×10^{-6} M) as a function of (a) Triton X and (b) Tween concentrations.

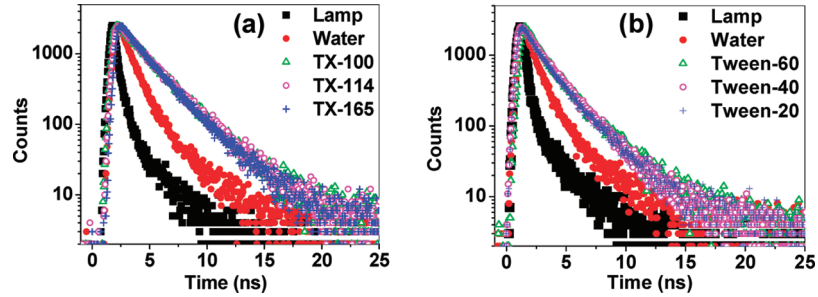

Figure 7. Time-resolved fluorescence decays of AODIQ in aqueous micellar media (λ_{exc} = 403 nm) in the case of (a) Triton X series and (b) Tween series of surfactants. The sharp profile on the left is the lamp profile.

Time-Resolved Fluorescence Decay. Fluorescence lifetime often serves as an excellent indicator to pinpoint the location of the probe in a multicomponent environment. Differential degrees of solvent relaxation around the fluorophore and/or partitioning of the fluorophore in distinct regions of a confined environment give rise to differences in the fluorescence lifetime of the fluorophore. AODIQ shows biexponential decays both in aqueous and in micellar environments. In aqueous solution, the existence of different hydrogen bonded species formed with the surrounding solvent molecules has often been ascribed to be responsible for such multiexponential decay behavior.[20] Figure 7 depicts the decay profiles of AODIQ in aqueous and micellar environments. The lifetime values of the probe in the micellar environments are remarkably longer than those in pure aqueous solution. Within Triton X or Tween series, however, the fluorescence lifetime of AODIQ does not differ remarkably with a change in the surfactant chain length.

The multiexponential decay of a polarity sensitive probe molecule may originate from the location of the probe in different polarity regions. That superposition of many decays of slightly different lifetimes looks like biexponential decay has been discussed by many authors.[39−41] However, we have yet to rationalize the biexponential decay of AODIQ in water. Maybe the probe, containing so many heteroatoms, undergoes unequal hydration. All lifetime values of the fluorophore are collected in Table 3. Extraction of meaningful rate constants in such heterogeneous systems is difficult. Instead of placing too much emphasis on the magnitudes of the individual decay constants in such complex decays, we chose to use the mean fluorescence lifetime that serves as an important parameter for exploiting the dynamical behavior of AODIQ in these micellar environments.

TABLE 3: Fluorescence Lifetimes of AODIQ in Aqueous and Micellar Environments

environment	a_1	τ_1 (ns)	a_2	τ_2 (ns)	$\langle\tau_f\rangle$ (ns)	χ^2
water	0.91	0.84	0.09	2.58	1.25	1.01
TX-114 (2.0 mM)	0.66	1.97	0.34	3.32	2.60	1.01
TX-100 (2.5 mM)	0.51	1.74	0.49	3.03	2.55	1.11
TX-165 (3.0 mM)	0.60	1.65	0.40	2.99	2.38	1.09
Tween-20 (0.25 mM)	0.58	1.13	0.42	2.56	2.02	1.12
Tween-40 (0.20 mM)	0.63	1.18	0.37	2.72	2.06	1.06
Tween-60 (0.22 mM)	0.54	1.25	0.46	2.73	2.12	1.11

The discussion so far reports that the probe binds with the micelles in a region where the polarity is less than that of bulk water. The decreased polarity around the probe in the micellar environments is also reflected in an increase in the fluorescence lifetime. In nonpolar 1,4-dioxane the fluorescence lifetime of AODIQ is found to be very short (~0.1 ns), and it differs appreciably from the lifetimes (~2 ns) estimated in the micellar systems. As the core of the micelle resembles more or less 1,4-dioxane,[11] the observation negates the location of the probe in the core region. The observed lifetimes are comparable to that

TABLE 4: Dynamic Parameters of Fluorescence Anisotropy of AODIQ in Micelles

environment	r_h (nm)	r_0	a_{1r}	τ_{1r} (ps)	a_{2r}	τ_{2r} (ns)	χ^2	$\langle\tau_r\rangle$ (ns)
water		0.40	1.0	146 ± 70			1.12	0.146
TX-114	4.5	0.39	0.59	104 ± 61	0.41	4.23 ± 0.08	1.06	1.80
TX-100	4.1	0.38	0.59	104 ± 64	0.41	3.28 ± 0.07	1.01	1.39
TX-165	3.8	0.40	0.49	130 ± 61	0.51	2.33 ± 0.09	1.05	1.26
Tween-20	4.8	0.38	0.48	123 ± 77	0.52	1.49 ± 0.08	1.12	0.87
Tween-40	5.0	0.39	0.36	114 ± 78	0.64	1.71 ± 0.09	1.11	1.14
Tween-60	8.4	0.39	0.45	133 ± 74	0.55	2.35 ± 0.07	1.13	1.35

in a water−alcohol mixture, indicating that the probable location of the fluorophore is the micelle−water interface. A slight difference in the measured lifetimes in water to micelles can be explained by considering the effect of polarity on the fluorescence lifetime of AODIQ.[8,11]

With an increase in the PEO chain length, the average lifetime value decreases. A reverse trend is observed in the $\langle\tau_f\rangle$ value on increasing the alkyl chain length. A probable argument in this regard may be derived from the variation of hydrophobicity and hydrophilicity in the micelles with a change of the surfactant chain lengths. As the number of PEO groups increase in the surfactant chain, the micellar palisade layer experiences an increase in polarity due to increased water penetration. Literature reports that the microviscosity in the palisade layer of TX-165 micelles is about 32% lower than that of TX-100 micelles.[9] Our microviscosity determination results also confirm this conjecture. The microviscosity of TX-114 is even higher than TX-100. Thus, it is expected that the water structure in the palisade layer of the TX-165 micelle will be relatively loose and have a higher degree of hydration compared to TX-100 and TX-114. This results in a lowering in the lifetime values with increasing PEO chain length. The marginal increase in the fluorescence lifetime of the probe in Tween series micelles with an increase in the alkyl chain length is rationalized from an increase in the rigidity of the microenvironment around the fluorophore.

Dynamic Light Scattering. Dynamic light scattering (DLS) measurement provides an effective way to investigate the dimensions of macromolecular and supramolecular assemblies.[42,43] It estimates the diffusion coefficient from which the hydrodynamic radius of the particle (r_h) can be extracted using the Stokes−Einstein equation assuming the assembly to be spherical.[44,45] The distribution was found to be fairly monomodal and the hydrodynamic radii obtained from the DLS measurements are given in Table 4. It was also noticed that upon addition of the probe to each of the micellar solutions there was hardly any change in the hydrodynamic radii.

Time-Resolved Fluorescence Anisotropy. To obtain further insight into the microenvironment around the probe, time-resolved fluorescence anisotropy studies of AODIQ in aqueous and in micellar environments were performed. The time dependent decay of the fluorescence anisotropy provides additional information about the rotational motion and/or rotational relaxation of the fluorophore in organized assemblies. In pure aqueous medium the anisotropy decay is found to be single exponential while in the micellar media the decay characteristics comprise biexponential components. Figure 8 illustrates the fluorescence anisotropy decays of AODIQ in aqueous and aqueous micellar solutions.

The functional form of the biexponential anisotropy decay $r(t)$ in micelles can be represented as

$$r(t)=r_0[a_{1r}\exp(-t/\tau_{1r}) + a_{2r}\exp(-t/\tau_{2r})] \quad (7)$$

where r_0 is the limiting anisotropy that describes the inherent depolarization of a given molecule, τ_{1r} and τ_{2r} are the two rotational relaxation times of the probe in micelles, a_{1r} and a_{2r} are the pre-exponents that provide the fraction of the two reorientation times. All the anisotropy decay parameters in aqueous as well as aqueous micellar environments are collected in Table 4. It is pertinent to mention here that a small scatter contribution might be responsible for the high r_0 values. It, however, does not contribute toward the determined dynamical parameters.

A quick look at the results shows that the AODIQ molecule exhibits a much slower fluorescence anisotropy decay in the micellar environments as compared to that in pure water. In pure water the rotational relaxation time of the AODIQ probe is obtained as 146 ps. In micelles the fluorescence anisotropy decays are biexponential. The shorter component is close to the reorientation time of the probe in aqueous medium whereas the longer component is significantly higher. This indicates that the AODIQ molecule experiences motionally restricted environments in the micelles. Thus, there is an increase of microviscosity for the probe surrounding the micelles compared to that in free aqueous medium. The average rotational relaxation times ($\langle\tau_r\rangle$) were calculated using eq 5 and are given in Table 4.

In micelles, biexponential anisotropy decay of AODIQ invite several arguments. One obvious possibility is that the short and long components in the anisotropy decay arise from the rotational diffusion of the free dye in solution and micelle-bound dye, respectively. In the course of checking the validity

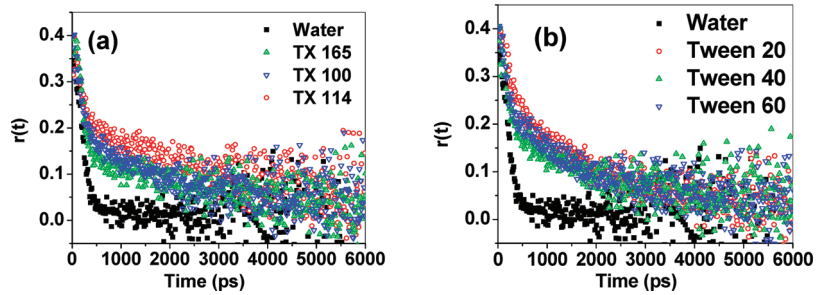

Figure 8. Fluorescence anisotropy decays of AODIQ (3×10^{-6} M) in water and in aqueous micellar media of (a) Triton X series and (b) Tween series of surfactants. $\lambda_{exc} = 403$ nm.

SCHEME 3: *Two-Step and Wobbling in a Cone* Model of Rotational Dynamics

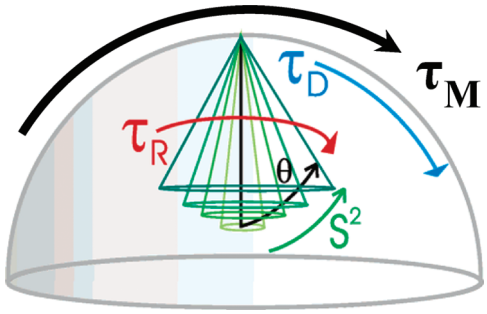

of this consideration, using merocyanine 540, Quitevis *et al.*[46] calculated the equilibrium constant for free and micelle-bound probe interconversion and thereby found the ratio of the free and the bound probe. In a similar manner, we calculated the ratio of concentration of the free to the micelle-bound fluorophore and it was found to be enormously low. This observation compels us to conclude that the anisotropy decay in the micellar environments is only due to the dynamics of the dye bound to micelles and the free dye does not put a signature on it.[46] Another possible explanation of the biexponential anisotropy decay is ascribed to the rotational diffusion of the dye bound to two different sites (headgroup region and core region) within the micelle. In micelles, the region of high viscosity is known to be the core region.[8,11] The studies relating to micropolarity, as discussed above, reveal that AODIQ resides mostly in the water−micelle interfacial zone. Also, a higher population in the core region is not physically reasonable for an ICT probe like AODIQ, containing so many heteroatoms. Again, in the photoexcited state the probe is significantly charged and hence is expected to be at the surface of the micellar units. A detailed fluorescence quenching study using ionic quencher in different micelles has also revealed that the probe molecule resides at the micellar surface. So in tune with the numerous studies in the literature[16,41,43−48] it can be said that the biexponential anisotropy decay in the present study is not due to the fact that the probe is solubilized in two distinct regions of the micelles. Invalidating all these options we try to explain the observed biexponential decay in terms of the probe undergoing different kinds of rotational motions in the micellar media. Such a behavior is often explained using the *two-step and wobbling in a cone* model.[43−49] In micellar solution with the probe in the micellar palisade layer, three different kinds of motions can contribute to the observed decay patterns.[4,42] These are (i) the wobbling motion of the probe within the micellar palisade layer, (ii) the lateral diffusion of the probe along a spherical surface, and (iii) rotational motion of the whole micelle containing the probe.[4,9,42] The observed biexponential behavior of $r(t)$ is ascribed to the interplay of all these motions. According to the two-step and wobbling in a cone model, the probe molecules undergo slow lateral diffusion on the surface of the micelle and also fast wobbling motion in the micelle that are coupled to the rotation of the micelle as a whole (Scheme 3).

Several rotational parameters for the present probe have been determined using this model in the studied nonionic micelles. Experimentally measured τ_{1r} and τ_{2r} are related to the time constants for lateral diffusion τ_D, wobbling motion τ_W, and the overall rotation of the micelle τ_M by the following relations.[43−48]

$$1/\tau_{2r} = 1/\tau_D + 1/\tau_M \quad (8)$$

$$1/\tau_{1r} = 1/\tau_W + 1/\tau_{2r} \quad (9)$$

where τ_{1r} and τ_{2r} are the observed fast and slow components. The data are summarized in Table 5. Overall rotation of the micelles can be estimated by using the Stokes−Einstein−Debye equation

$$\tau_M = 4\eta\pi r_h^3/3kT \quad (10)$$

where η is the viscosity of water in poise, r_h is the hydrodynamic radius of the micelles,[50] and k and T are the Boltzmann constant and absolute temperature, respectively. Besides the dynamical parameters, we have further calculated the generalized order parameter (S) using the following equation to realize the information about the motional restriction on the probe molecule.

$$S^2 = a_{2r} \quad (11)$$

The order parameter, S, is a measure of spatial restriction and has values from 0 (for unrestricted motion) to 1 (for complete restriction on the motion). All the dynamical parameters are tabulated in Table 5.

With a glance at the data presented in Tables 4 and 5 one realizes that the time constants for the overall rotation of the micelle (τ_M) are significantly larger than the slower component of the time constant (τ_{2r}) in the anisotropy decay, i.e., $\tau_M \gg \tau_{2r}$ while τ_D and τ_{2r} are almost identical. Before we proceed further with the analysis, it is important to note that the observation of the biexponential anisotropy decay does not necessarily mean the prevalence of lateral diffusion of the probes. However, in the absence of such processes, the slower component of the time constant should represent the time constant for the overall rotation of the micelle (τ_M). As mentioned, comparison of the values of τ_{2r} and τ_M for AODIQ confirms $\tau_M \gg \tau_{2r}$, suggesting that the lateral diffusion is indeed an important mechanism for the anisotropy decay of AODIQ. Since $\tau_M \gg \tau_{2r}$ (i.e., τ_{slow}), τ_{2r} essentially represents τ_D. The τ_D value in all the Triton X and Tween micelles is significantly longer. The probable cause of this longer rotational time may be ascribed to some specific interaction, possibly hydrogen bonding between the headgroup of the nonionic surfactants and the heteroatoms of the probe molecule, resulting in some hindrance in the rotational dynamical behavior. That the shape of the micelle is not changing can be argued from the fact that we observe a graded change in the rotational dynamics parameters, which would have not been so if there had been a change in the shape of the micelles. The DLS studies also certify that the shape of the micelles remains spherical even upon interaction with the probe, since insignificant change was observed in the hydrodynamic radii upon addition of AODIQ to the micelles when compared to the free micellar solutions.

The order parameter, S, of the probe in water is zero because the dye molecule tumbles freely and the distribution of the probe

TABLE 5: Rotational Parameters of AODIQ in Micelles Considering the *Two-Step and Wobbling in a Cone* Model

systems	r_h (nm)	τ_M (ns)	τ_D (ns)	τ_W (ps)
TX-114	4.5	83.1 ± 0.08	4.4 ± 0.08	235 ± 61
TX-100	4.1	62.8 ± 0.07	3.5 ± 0.07	107 ± 64
TX-165	3.8	50.0 ± 0.09	2.4 ± 0.09	137 ± 61
Tween-20	4.8	100.8 ± 0.08	1.5 ± 0.08	134 ± 77
Tween-40	5.0	113.9 ± 0.09	1.7 ± 0.09	122 ± 78
Tween-60	8.4	540.3 ± 0.07	2.3 ± 0.07	141 ± 74

is completely random. Again, in the micellar core the order parameter is known to be very low (close to zero), since the wobbling motion of the probe is expected to be almost isotropic.[46,51] However, the order parameters in all the micellar media are found to be in the range 0.6−0.8. The substantially high values of the order parameters are therefore a supportive indication of the fact that the probe molecules are located in the micelle−water interfacial region, where the surfactant chains are arranged in a much more ordered manner, rather than the interior of the micelles. Motions of the headgroups in the vicinity of the probe molecule are also responsible for the observed slower dynamics of the fluorophore within the micelles.[13] Thus the size of the headgroups of the surfactants seems to have a strong influence on the relaxation dynamics. It is important to mention here that the average rotational relaxation times (Table 4) of AODIQ increase with increasing alkyl chain length of the surfactants and decrease with increasing PEO chain length of the surfactants. Steady-state and time-resolved fluorescence anisotropy studies indicate that the degree of restriction around the fluorophore follows the order TX-165 < TX-100 < TX-114 and Tween-20 < Tween-40 < Tween-60. Thus an increase in the alkyl chain length and/or decrease in the PEO chain length make the micelles more compact. This leads to a decrease of water−micelle interaction resulting in an enhancement in the hydrophobicity of the micellar palisade layer.

4. Conclusion

The photophysical and dynamical behavior of the nonionic fluorophore, AODIQ, have been explored using steady-state and time-resolved fluorescence and fluorescence anisotropy techniques. The fluorophore binds strongly with the micelles. Fluorometric, micropolarity, and time-resolved studies suggest that the probe molecule resides in the palisade layer of all the nonionic micelles studied. The experiments revealed modification of the photophysics of AODIQ by the conjugate effect of polarity and rigidity of the micellar environments with varying poly(ethylene oxide) chain length in the case of the Triton X series and the alkyl chain length in the case of the Tween series of surfactants. Steady-state anisotropy results reveal that the motional restriction increases with an increase in the alkyl chain length and/or decrease in the PEO chain length. Time-resolved fluorescence anisotropy measurements corroborate it further. Various parameters related to the rotational motion of the fluorophore in the micelles have been determined using the *two-step and wobbling in a cone* model. The substantially high values of the order parameter, obtained from time-resolved anisotropy experiments, assign the location of the probe molecules in the micelle−water interface rather than the interior of the micelles. The significant feature of the present study is that the motional restriction decreases with an increase in the poly(ethylene oxide) chain length while it increases with an increase in the alkyl chain length.

Acknowledgment. Financial support from DBT and C.S.I.R., Government of India, is gratefully acknowledged. A.M., D.S., and A.G. thank CSIR for their research fellowships/associateship. D.B. thanks UGC for her research fellowship. We appreciate the cooperation received from Prof. C. R. Sinha and P. Dutta of our university, Prof. N. Sarkar and Dr. D. Seth of IIT Kharagpur, and Prof. K. P. Das and V. Banerjee of Bose Institute, Kolkata, for their kind help in the steady-state and time-resolved fluorescence anisotropy measurements and DLS studies respectively.

References and Notes

(1) Rosen, M. J. *Surfactant and Interfacial Phenomena*; Wiley Interscience: New York, 1978.
(2) Fendler, H. J.; Fendler, J. E. *Catalysis in Micellar and Macromolecular Systems*; Academic: New York, 1975.
(3) Tamoto, Y.; Segawa, H.; Shirota, H. *Langmuir* **2005**, *21*, 3757.
(4) Maiti, N. C.; Krishna, M. M. G.; Brito, P. J.; Periasamy, N. *J. Phys. Chem. B* **1997**, *101*, 11051.
(5) Hobbs, H. R.; Thomas, N. R. *Chem. Rev.* **2007**, *107*, 2786.
(6) Saroja, G.; Ramachandram, B.; Saha, S.; Samanta, A. *J. Phys. Chem. B* **1999**, *103*, 2906.
(7) Gehlen, M. H.; De Schryver, F. C. *Chem. Rev.* **1993**, *93*, 199.
(8) Mallick, A.; Haldar, B.; Maiti, S.; Chattopadhyay, N. *J. Colloid Interface Sci.* **2004**, *278*, 215.
(9) Kumbhakar, M.; Nath, S.; Mukherjee, T.; Pal, H. *J. Chem. Phys.* **2004**, *121*, 6026.
(10) Chakrabarty, D.; Chakraborty, A.; Seth, D.; Hazra, P.; Sarkar, N. *J. Chem. Phys.* **2004**, *122*, 184516.
(11) Das, P.; Mallick, A.; Haldar, B.; Chakrabarty, A.; Chattopadhyay, N. *J. Chem. Phys.* **2006**, *125*, 044516.
(12) Dutta Chowdhury, S.; Kumbhakar, M.; Nath, S.; Sarkar, S. K.; Mukherjee, T.; Pal, H. *J. Phys. Chem. B* **2007**, *111*, 8842.
(13) Chakrabarty, D.; Hazra, P.; Sarkar, N. *J. Phys. Chem. A* **2003**, *107*, 5887.
(14) Balabai, N.; Linton, B.; Napper, A.; Priyadarshy, S.; Sukharevsky, A. P.; Waldeck, D. H. *J. Phys. Chem. B* **1998**, *102*, 9617.
(15) Dutta, P.; Sen, P.; Mukherjee, S.; Bhattacharyya, K. *Chem. Phys. Lett.* **2003**, *382*, 426.
(16) Dutt, G. B. *J. Phys. Chem. B* **2003**, *107*, 3131.
(17) Becher, P. *J. Colloid Sci.* **1961**, *16*, 49.
(18) Saito, Y.; Sato, T. *J. Phys. Chem.* **1985**, *89*, 2110.
(19) Mallick, A.; Maiti, S.; Haldar, B.; Purkayastha, P.; Chattopadhyay, N. *Chem. Phys. Lett.* **2003**, *371*, 688.
(20) Mallick, A.; Haldar, B.; Chattopadhyay, N. *J. Phys. Chem. B* **2005**, *109*, 14683.
(21) Das, P.; Chakrabarty, A.; Haldar, B.; Mallick, A.; Chattopadhyay, N. *J. Phys. Chem. B* **2007**, *111*, 7401.
(22) Mallick, A.; Haldar, B.; Maiti, S.; Bera, S. C.; Chattopadhyay, N. *J. Phys. Chem. B* **2005**, *109*, 14675.
(23) Das, P.; Sarkar, D.; Chattopadhyay, N. *Chem. Phys. Lipids* **2008**, *154*, 38.
(24) (a) Mallick, A.; Mandal, M. C.; Haldar, B.; Chakrabarty, A.; Das, P.; Chattopadhyay, N. *J. Am. Chem. Soc.* **2006**, *128*, 3126. (b) Mallick, A.; Mandal, M. C.; Haldar, B.; Chakrabarty, A.; Das, P.; Chattopadhyay, N. *J. Am. Chem. Soc.* **2006**, *128*, 10629.
(25) Partearroyo, M. A.; Alonso, A.; Goni, F. M.; Tribout, M.; Paredes, S. *J. Colloid Interface Sci.* **1996**, *178*, 156.
(26) Heredia, A.; Bukovac, M. J. *J. Agric. Food Chem.* **1992**, *40*, 2290.
(27) Bhattacharyya, S. C.; Das, H.; Moulik, S. P. *J. Photochem. Photobiol. A: Chem.* **1993**, *74*, 239.
(28) Lee, M. S.; Park, S. S.; Lee, G. D.; Ju, C. S.; Hong, S. S. *Catal. Today* **2005**, *101*, 283.
(29) Giri, V. S.; Maiti, B. C.; Pakrashi, S. C. *Heterocycles* **1984**, *22*, 233.
(30) Demas, J. N.; Crosby, G. A. *J. Phys. Chem.* **1971**, *75*, 991.
(31) Lakowicz, J. R. *Principles of Fluorescence Spectroscopy*, 3rd ed.; Plenum: New York, 2006.
(32) Bhattachryya, K.; Chowdhury, M. *Chem. Rev.* **2003**, *93*, 507.
(33) Reichardt, C., Ratajazak, H., Orville-Thomas, W. J., Eds. *Molecular Interactions*; Wiley: New York, 1982; Vol. 3, p 255.
(34) Reichardt, C. *Chem. Rev.* **1994**, *94*, 2319.
(35) Kosower, E. M.; Dodiuk, H.; Tanizawa, K.; Ottolenghi, M.; Orbach, N. *J. Am. Chem. Soc.* **1975**, *97*, 2167.
(36) Chakrabarty, A.; Das, P.; Mallick, A.; Chattopadhyay, N. *J. Phys. Chem. B* **2008**, *112*, 3684.
(37) Muller, N. In *Reaction Kinetics in Micelles*; Cordes, E. A., Ed.; Plenum Press: New York, 1973.
(38) Berr, S.; Jones, R. R. M.; Johnson, J. S. *J. Phys. Chem.* **1992**, *96*, 5611.
(39) Cho, C. H.; Chung, M.; Lee, J.; Nguyen, T.; Singh, S.; Vedamulthu, M.; Yao, S.; Zhu, S. B.; Robinson, G. W. *J. Phys. Chem.* **1995**, *99*, 7806.
(40) Toptygin, D.; Svodova, J.; Konopasek, I.; Brand, L. J. *J. Chem. Phys.* **1992**, *96*, 7919.
(41) Sen, S.; Sukul, D.; Dutta, P.; Bhattacharyya, K. *J. Phys. Chem. A* **2001**, *105*, 7495.
(42) Feitosa, E.; Brown, W.; Wang, K.; Barreleiro, P. C. A. *Macromolecules* **2002**, *35*, 201.
(43) Almgren, M.; Gimel, J. C.; Wang, K.; Karlsson, G.; Edward, K.; Brown, W. *J. Colloid Interface Sci.* **1998**, *202*, 222.
(44) Robert, P. *Dynamic Light Scattering: Applications of Photon Correlation Spectroscopy*; Plenum: New York, 1985.
(45) Brown, W. *Light Scattering*; Oxford University Press: Oxford, U.K., 1996.

(46) Quitevis, E. L.; Marcus, A. H.; Fayer, M. D. *J. Phys. Chem.* **1993**, *97*, 5762.
(47) Lipari, G.; Szabo, A. *Biophys. J.* **1980**, *30*, 489.
(48) Chakrabarty, A.; Seth, D.; Setua, P.; Sarkar, N. *J. Chem. Phys.* **2006**, *124*, 74512.
(49) Kinosita, K.; Kawato, S.; Ikegami, A. *Biophys. J.* **1977**, *20*, 289.
(50) Dutt, G. B. *J. Phys. Chem. B* **2004**, *108*, 3651.
(51) Ahlls, T.; Smerman, O.; Hjelm, C.; Lindman, B. *J. Phys. Chem.* **1983**, *87*, 822.

JP900575E